BELLE2-NOTE-PL-2020-018
DRAFT Version 1.0
July 27, 2020

Belle II experiment sensitivity to the LFV decay $\tau \to e + \alpha$

The Belle II Collaboration

Abstract

We study the charged lepton flavor violating decay $\tau \to e\alpha$, where α is a non-standard invisible boson that leaves the Belle II detector undetected. This Note presents plots showing the optimization procedure, relevant observables, and upper limit estimates using Belle II simulated data, assuming no $\tau \to e\alpha$ signal in 25 fb^{-1} of integrated luminosity. Further work is in progress in order to include systematic uncertainties.

Contents

1. Introduction 3

2. Background suppression 4
2.1. Distributions used for optimization 4
2.2. Distributions after "N-1" requirements 5
2.3. Distributions after selection optimization 6

3. τ pseudo-rest frame and thrust frame 7

4. Upper limit estimation 8

References 8

1. INTRODUCTION

We present preliminary Monte Carlo studies on the search for $\tau \to \ell\alpha$ decays, where ℓ is either a electron or a muon, and α is a particle that escapes the Belle II detector undetected. This is a charged Lepton Flavor Violating (LFV) process not present in the Standard Model of particle physics (SM), but appears in various new physics models [1–8]. For a massless α particle, the current limits at 95 % C.L. are $Br(\tau \to e\alpha)/Br(\tau \to e\nu\overline{\nu}) < 1.5\%$ and $Br(\tau \to \mu\alpha)/Br(\tau \to \mu\nu\overline{\nu}) < 2.6\%$, as reported by the ARGUS Collaboration [9].

The search is based on measuring the production of LFV $\tau \to \ell\alpha$ decays with respect to the SM process $\tau \to \ell\nu_l\nu_\tau$. In the present study, only the electron decay channels are considered.

Figure 2.1.1 presents the three distributions used for signal optimization in simulated data, after requiring standard selection criteria on the reconstructed objects. To observe the effect of the requirements found in the optimization, Fig. 2.2.1 shows each of these distributions after applying the optimized criteria to the complementary distributions. Figure 2.3.1 presents the distributions after all selection requirements.

The measurement is performed in the so called pseudo-rest frame, a technique developed by ARGUS [9]. Section 3 presents the relevant distributions used for this measurement, including a modification of the ARGUS method that uses the thrust vector to estimate the direction of the τ lepton.

Finally, for 25 fb^{-1} of data, Fig. 4.0.1 shows the expected 95 % C.L. upper limits on $Br(\tau \to e\alpha)/Br(\tau \to e\nu\overline{\nu})$ for different masses of the α particle. Table I summarizes these results.

2. BACKGROUND SUPPRESSION

2.1. Distributions used for optimization

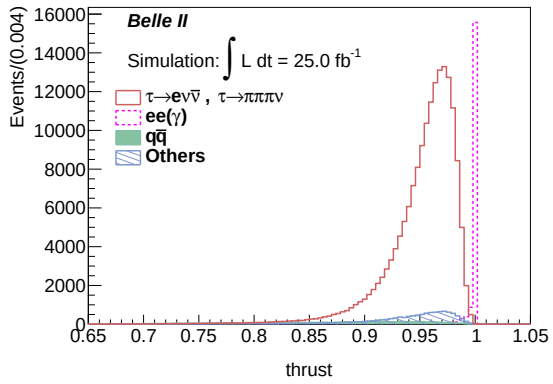

(a) Thrust of the event.

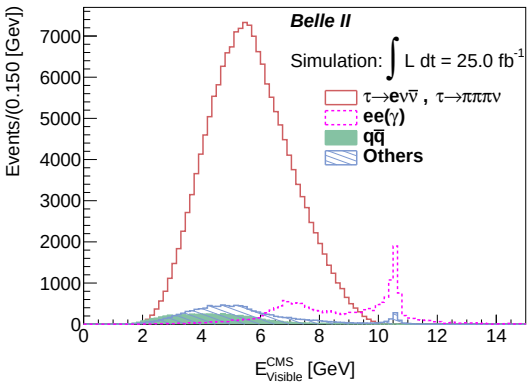

(b) Visible energy of the event.

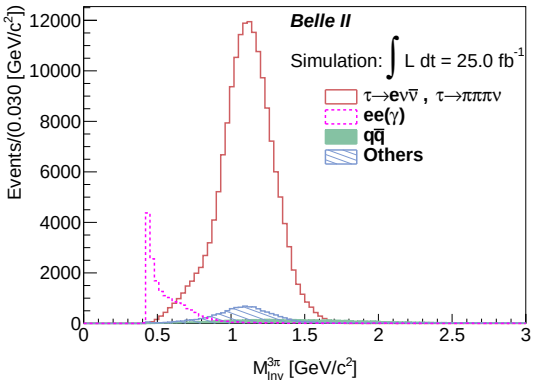

(c) Invariant mass of the 3-prong system.

FIG. 2.1.1: Event distributions for reconstructed 3x1-prong decays. The 3x1-prong topology is obtained by means of the thrust vector ($\widehat{n}_{thrust}$, defined below), which is used to separate the event into signal (1-prong) and tag (3-prong) hemispheres. Candidate events are identified with the tag side τ decaying into into three charged pion candidates, $\tau \to \pi\pi\pi\nu$, and with the signal side τ decaying into one electron candidate, $\tau \to e\nu\bar{\nu}$. Neutrinos are not reconstructed. Shown are: a) the event thrust distribution, defined as $T = \sum_i \frac{|\overrightarrow{p}_i^{CMS} \cdot \widehat{n}_{thrust}|}{\sum |\overrightarrow{p}_i^{CMS}|}$, where $\overrightarrow{p}_i^{CMS}$ is the momentum in the center-of-mass frame of the i-th reconstructed particle in the event (tracks and photons), and $\widehat{n}_{thrust}$ is the (thrust) direction that maximizes the sum; b) the event visible energy calculated from tracks and photons; and c) the invariant mass of the 3-prong system, $M_{Inv}^{3\pi} = \sqrt{E_{3\pi}^2 - p_{3\pi}^2}$.

2.2. Distributions after "N-1" requirements

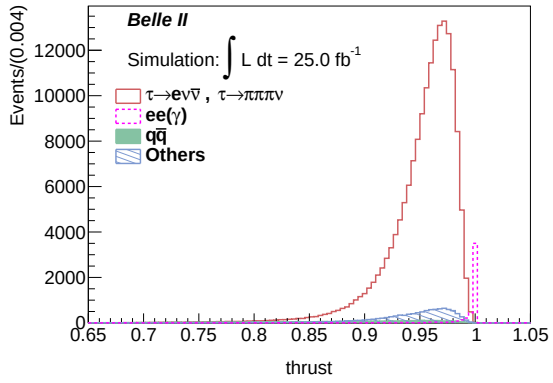

(a) Thrust of the event.

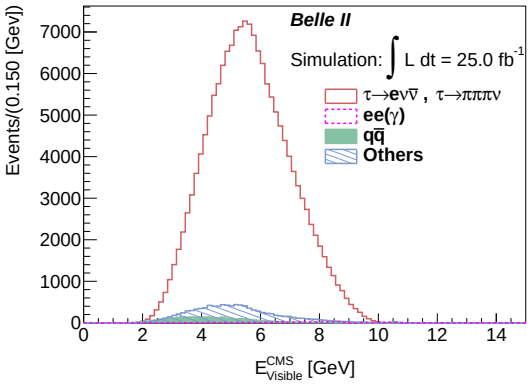

(b) Visible energy of the event.

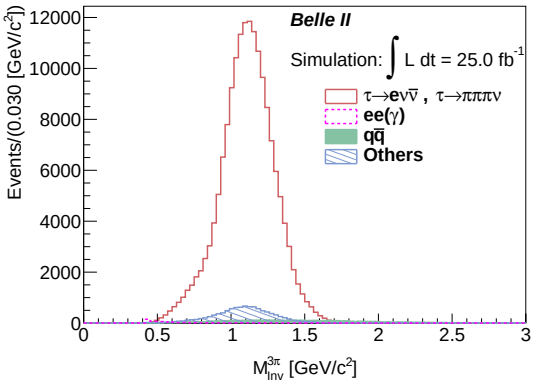

(c) Invariant mass of the 3-prong system.

FIG. 2.2.1: Same distributions as in Fig. 2.1.1, each of them with additional requirements on the other two variables. These requirements are obtained from a selection optimization that maximizes the significance of $\tau \to e\nu\bar{\nu}$ decays, using the figure of merit $\frac{S}{\sqrt{S+B}}$. S is the number of $\tau \to e\nu\bar{\nu}$ events, and B the number of remaining SM ($ee, q\bar{q}$, others) background events. Shown are: a) the event thrust, with 2.0 GeV $< E^{CMS}_{Visible} <$ 9.9 GeV and 0.48 GeV/c^2 $< M^{3\pi}_{Inv} <$ 1.66 GeV/c^2; b) the event visible energy, with 0.8 $<$ thrust $<$ 0.99 and same invariant mass requirement as in a); and c) the invariant mass of the 3-prong system, with the same requirements on thrust and visible energy as in b) and a), respectively.

2.3. Distributions after selection optimization

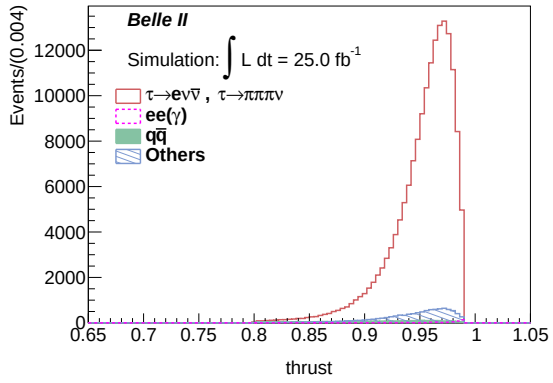

(a) Thrust of the event.

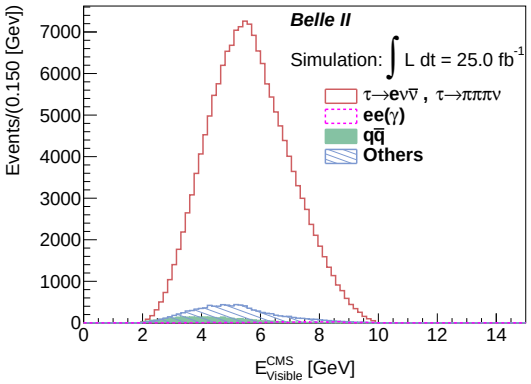

(b) Visible energy of the event.

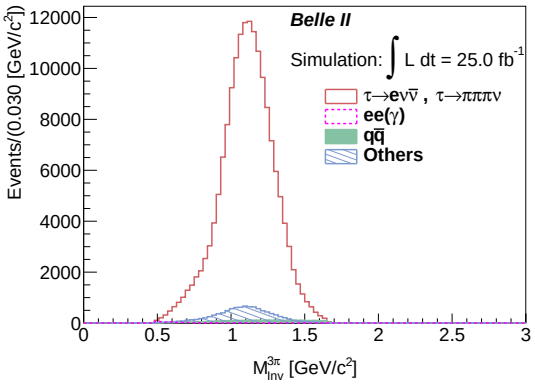

(c) Invariant mass of the 3-prong system.

FIG. 2.3.1: Same distributions as in Fig. 2.2.1 after all selection requirements: 2.0 GeV $< E^{CMS}_{Visible} <$ 9.9 GeV, 0.48 GeV/c^2 $< M^{3\pi}_{Inv} <$ 1.66 GeV/c^2, and 0.8 $<$ thrust $<$ 0.99. Shown are: a) the event thrust; b) the event visible energy; and c) the inviariant mass of the 3-prong system.

3. τ PSEUDO-REST FRAME AND THRUST FRAME

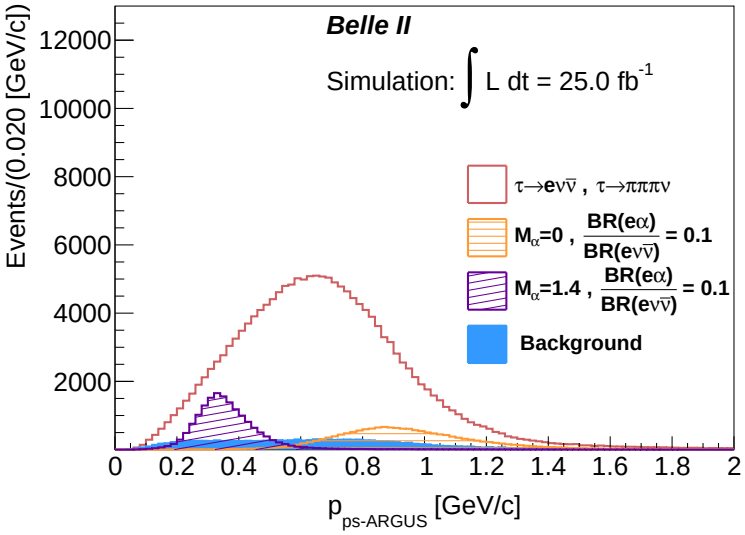

(a) Argus method.

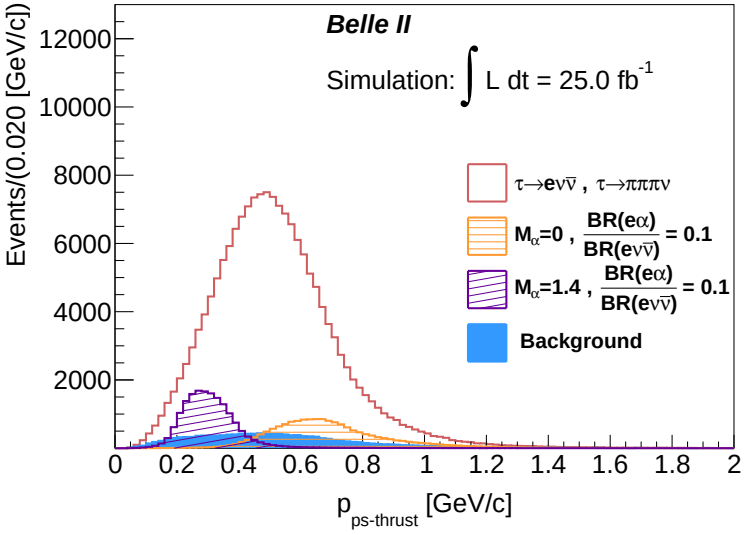

(b) Thrust method.

FIG. 3.0.1: Electron momentum distributions in the τ "pseudo-rest" frame obtained from simulated data after all selection requirements described in Fig. 2.3.1. Shown are the contributions from $\tau \to e\nu\bar{\nu}$ (signal) decays and the remaining SM background. Distributions of non-standard decays, $\tau \to e\alpha$, are also shown for masses $M_\alpha = 0$ and 1.4 GeV/c^2, assuming $\mathcal{B}(\tau \to e\alpha)/\mathcal{B}(\tau \to e\nu\nu) = 0.1$. The Lorentz boost of the electron to the signal τ rest frame must be approximated, since neither the neutrino (in the tag side) nor the α (in the signal side) can be detected in order to reconstruct completely neither τ: a) in the Argus method, the direction of the signal τ is approximated to the direction of the total momentum of the 3-prong system, $\vec{e}_\tau \approx -\vec{e}_{3h}$, while its energy is fixed to the energy of one electron beam in the center-of-mass frame, $E_\tau = E_{beam}$; b) in the Thrust method, the direction of the signal τ is approximated to the direction of the event thrust vector, $\vec{e}_\tau \approx \hat{n}_{thrust}$, and $E_\tau = E_{beam}$.

4. UPPER LIMIT ESTIMATION

Mass (α) [GeV/c^2]	ARGUS (1995)	Argus method	Thrust method
0	0.015	0.0025	0.0016
0.5	0.017	0.0028	0.0025
0.7	0.024	0.003	0.0031
1.0	0.036	0.004	0.004
1.2	0.034	0.005	0.005
1.4	0.025	0.003	0.004
1.6	0.006	0.001	0.0009

TABLE I: Upper limits for $\mathcal{B}(\tau \to e\alpha)/\mathcal{B}(\tau \to e\nu\nu)$ published by the ARGUS Collaboration [9] and current estimates using $L_{int} = 25$ fb^{-1} of simulated Belle II data. Upper limits are calculated at 95% C.L. Current estimates use the asymptotic formulation [10] of the CL_s method [11]. No systematic uncertainties are included.

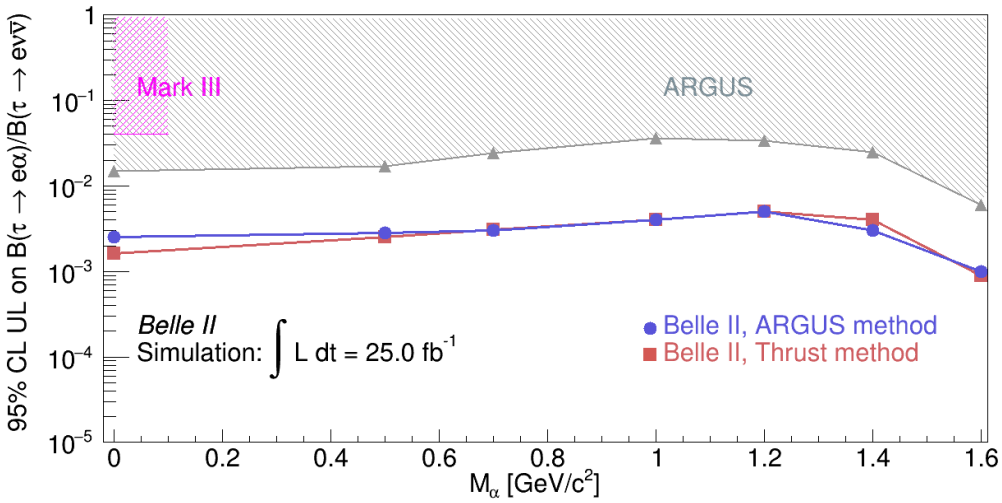

FIG. 4.0.1: 95% C.L. upper limit estimations for $\mathcal{B}(\tau \to e\alpha)/\mathcal{B}(\tau \to e\nu\nu)$ using the Argus and Thrust methods, assuming 25 fb^{-1} of Belle II simulated data. Previous experimental results from the ARGUS [9] and Mark III [12] collaborations are also shown. Belle II estimates are based on an asymptotic implementation of the CL_s technique. No systematic uncertainties are included.

[1] Kento Asai, Koichi Hamaguchi, Natsumi Nagata, Shih-Yen Tseng, and Koji Tsumura. Minimal Gauged U(1)$_{L_\alpha - L_\beta}$ Models Driven into a Corner. 2018.

[2] Julian Heeck and Werner Rodejohann. Lepton Flavor Violation with Displaced Vertices. *Phys. Lett.*, B776:385–390, 2018.

[3] Fredrik Björkeroth, Eung Jin Chun, and Stephen F. King. Flavourful Axion Phenomenology. *JHEP*, 08:117, 2018.

[4] Wolfgang Altmannshofer, Chien-Yi Chen, P. S. Bhupal Dev, and Amarjit Soni. Lepton flavor violating Z explanation of the muon anomalous magnetic moment. *Phys. Lett.*, B762:389–398, 2016.

[5] Camilo Garcia-Cely and Julian Heeck. Neutrino Lines from Majoron Dark Matter. *JHEP*, 05:102, 2017.

[6] Oz Davidi, Rick S. Gupta, Gilad Perez, Diego Redigolo, and Aviv Shalit. The hierarchion, a relaxion addressing the Standard Model's hierarchies. *JHEP*, 08:153, 2018.

[7] Jonathan L. Feng, Takeo Moroi, Hitoshi Murayama, and Erhard Schnapka. Third generation familons, b factories, and neutrino cosmology. *Phys. Rev.*, D57:5875–5892, 1998.

[8] Francesco D'Eramo, Ricardo Z. Ferreira, Alessio Notari, and José Luis Bernal. Hot Axions and the H_0 tension. *JCAP*, 1811(11):014, 2018.

[9] H. Albrecht et al. A Search for lepton flavor violating decays $\tau \to e\alpha$, $\tau \to \mu\alpha$. *Z. Phys.*, C68:25–28, 1995.

[10] Glen Cowan, Kyle Cranmer, Eilam Gross, and Ofer Vitells. Asymptotic formulae for likelihood-based tests of new physics. *Eur. Phys. J. C*, 71:1554, 2011.

[11] A L Read. Presentation of search results: the CL_s technique. *Journal of Physics G: Nuclear and Particle Physics*, 28(10):2693–2704, Sep 2002.

[12] Baltrusaitis R M and others. τ leptonic branching ratios and a search for goldstone-boson decay. *Phys. Rev. Lett.*, 55:1842–1845, Oct 1985.